

## CO<sub>2</sub> reduction on supported Ru/Al<sub>2</sub>O<sub>3</sub> catalysts: cluster size dependence of product selectivity

Ja Hun Kwak, Libor Kovarik, and Janos Szanyi

ACS Catal., Just Accepted Manuscript • DOI: 10.1021/cs400381f • Publication Date (Web): 16 Sep 2013

Downloaded from <http://pubs.acs.org> on September 27, 2013

### Just Accepted

"Just Accepted" manuscripts have been peer-reviewed and accepted for publication. They are posted online prior to technical editing, formatting for publication and author proofing. The American Chemical Society provides "Just Accepted" as a free service to the research community to expedite the dissemination of scientific material as soon as possible after acceptance. "Just Accepted" manuscripts appear in full in PDF format accompanied by an HTML abstract. "Just Accepted" manuscripts have been fully peer reviewed, but should not be considered the official version of record. They are accessible to all readers and citable by the Digital Object Identifier (DOI®). "Just Accepted" is an optional service offered to authors. Therefore, the "Just Accepted" Web site may not include all articles that will be published in the journal. After a manuscript is technically edited and formatted, it will be removed from the "Just Accepted" Web site and published as an ASAP article. Note that technical editing may introduce minor changes to the manuscript text and/or graphics which could affect content, and all legal disclaimers and ethical guidelines that apply to the journal pertain. ACS cannot be held responsible for errors or consequences arising from the use of information contained in these "Just Accepted" manuscripts.



ACS Publications  
High quality. High impact.

ACS Catalysis is published by the American Chemical Society, 1155 Sixteenth Street N.W., Washington, DC 20036

Published by American Chemical Society. Copyright © American Chemical Society. However, no copyright claim is made to original U.S. Government works, or works produced by employees of any Commonwealth realm Crown government in the course of their duties.

# CO<sub>2</sub> reduction on supported Ru/Al<sub>2</sub>O<sub>3</sub> catalysts: cluster size dependence of product selectivity

Ja Hun Kwak<sup>1\*#</sup>, Libor Kovarik<sup>2</sup>, and János Szanyi<sup>1\*</sup>

<sup>1</sup>Institute for Integrated Catalysis, <sup>2</sup>Environmental Molecular Sciences Laboratory, Pacific Northwest National Laboratory, Richland, WA 99352, USA

Corresponding authors: [jhkwak@unist.ac.kr](mailto:jhkwak@unist.ac.kr); [janos.szanyi@pnnl.gov](mailto:janos.szanyi@pnnl.gov)

<sup>#</sup>Current Address: School of Nano-Bioscience and Chemical Engineering, UNIST  
100 Banyeon-Ri, Ulsan 689-798, Korea:

## Abstract

The catalytic performance of a series of Ru/Al<sub>2</sub>O<sub>3</sub> catalysts with Ru content in the 0.1-5% range was examined in the reduction of CO<sub>2</sub> with H<sub>2</sub>. At low Ru loadings ( $\leq 0.5$  %) where the active metal phase is highly dispersed (mostly atomically) on the alumina support CO is formed with high selectivity. With increasing metal loading the selectivity toward CH<sub>4</sub> formation increases, while that for CO production decreases. In the 0.1% Ru/Al<sub>2</sub>O<sub>3</sub> catalyst Ru is mostly present in atomic dispersion as STEM images obtained from the fresh sample prior to catalytic testing reveal. STEM images recorded from this same sample following temperature programmed reaction test clearly show the agglomeration of small metal particles (and atoms) into 3D clusters. The clustering of the highly dispersed metal phase is responsible for the observed dramatic selectivity change during elevated temperature tests: dramatic decrease in CO, and large increase in CH<sub>4</sub> selectivity. Apparent activation energies, estimated from the slopes of Arrhenius plots, of 82 kJ/mol and 62 kJ/mol for CO and CH<sub>4</sub> formation were determined, respectively, regardless of Ru loading. These results suggest that the formation of CO and CH<sub>4</sub> follow different reaction pathways, or proceed on active centers of different nature. Reactions with CO<sub>2</sub>/H<sub>2</sub> and CO/H<sub>2</sub> mixtures (under otherwise identical reaction conditions) reveal that the onset temperature of CO<sub>2</sub> reduction is about 150 °C lower than of CO reduction.

Keywords: CO<sub>2</sub> reduction; Ru/Al<sub>2</sub>O<sub>3</sub>; CO/CH<sub>4</sub> selectivity; Ru dispersion; reaction mechanism

## Introduction

The conversion of CO<sub>2</sub> to high energy density organic molecules (e.g., methanol or methane) has been proposed over both homogeneous and heterogeneous catalysts containing transition metals (e.g., Cu, Ni and Pd) as active centers [1,2,3]. Considerable work has been aimed at designing and synthesizing heterogeneous CO<sub>2</sub> reduction catalysts [4,5,6,7,8]. The activity and selectivity of these catalysts have been shown to be very sensitive to the cluster size and the shape of the metal particles dispersed on the support, as well as to the interaction between the active metals and oxide supports [9, 10]. However, these features of oxide-supported metal catalysts remain, to a great extent, hard to control due to the nature of synthetic protocols, and, in particular, to sintering of metal clusters during the activation process. The heterogeneous catalytic conversion of CO<sub>2</sub> is currently not feasible due to the demanding reaction conditions (e.g., high catalyst bed temperature) originating from the chemical inertness of CO<sub>2</sub>. Therefore, understanding the elementary reaction steps of catalytic CO<sub>2</sub> reduction is critical in order to design economically viable catalytic systems.

Despite the ongoing research efforts, the role of support and the control of CO/CH<sub>4</sub> selectivity in the reduction of CO<sub>2</sub> with H<sub>2</sub> have not been well established, in particular not on sub-nanometer-sized supported metal atoms/clusters. Recently we have reported on the very unique catalytic properties of isolated Pd atoms in the reduction of CO<sub>2</sub> [11]. In that report, we showed that atomically dispersed supported metals can be catalytically active even in the demanding reaction of CO<sub>2</sub> reduction but their activity and selectivity patterns differ by a large extent from those of 3D metal particles. The results of CO<sub>2</sub> hydrogenation reaction on Pd/Al<sub>2</sub>O<sub>3</sub> and Pd/MWCNT catalysts have unambiguously proved the need of two different functionalities in an active catalyst. The reduction of CO<sub>2</sub> requires the presence of a catalyst component that is able to activate CO<sub>2</sub> (either the support oxide (Al<sub>2</sub>O<sub>3</sub>) or an oxide promoter), and a metallic component (here Pd) that is able to dissociate H<sub>2</sub>. When both of these functionalities are present, the CO and CH<sub>4</sub> selectivities seem to be determined by the sizes of the metal particles.

In this study we prepared a series of Ru on alumina catalysts with Ru loadings that assured a dispersion range from atomic to 3D clusters and tested their CO<sub>2</sub> reduction performances. Atomically dispersed Ru on alumina initially produced CO exclusively by CO<sub>2</sub> reduction. This is in complete contrast with the catalytic behavior of 3D Ru clusters supported on alumina that have been known to be efficient methanation catalysts [12,13,14]. Based on these

results we propose that CO can be produced by different reaction mechanisms on active Ru centers with different particle sizes. Furthermore, CO may not be a simple reaction intermediate in the path of CO<sub>2</sub> hydrogenation to CH<sub>4</sub>.

### Experimental:

Al<sub>2</sub>O<sub>3</sub>-supported, 0.1%, 0.5%, 1%, 2% and 5 wt% Ru catalysts were prepared on a commercial  $\gamma$ -Al<sub>2</sub>O<sub>3</sub> powder (Condea, BET surface area = 200 m<sup>2</sup>/g) by the incipient wetness method using ruthenium(III) nitrosyl nitrate solution (Ru(NO)(NO<sub>3</sub>)<sub>x</sub>(OH)<sub>y</sub>, x+y =3 in dilute nitric acid, 1.5% Ru, Aldrich) as the precursor.

CO<sub>2</sub> reduction activity measurements were conducted by a temperature programmed reaction methods in a packed bed reactor using 50 mg of catalyst powder samples (quartz reactor O.D. = 1/2"). The catalysts were activated prior to catalytic measurements by calcination at 500 °C for 2 h under 6.7 % O<sub>2</sub>/He (flow rate = 60 ml/min) and followed by reduction at 500 °C for 30 min under 15 % H<sub>2</sub>/He (flow rate = 60 ml/min). The activity was measured using a feed gas mixture containing 5 % CO<sub>2</sub> and 15% H<sub>2</sub> in He (total flow rate = 60 ml/min and H<sub>2</sub>/CO<sub>2</sub> = 3; m<sub>catalyst</sub> = 50 mg)). The concentrations of all reactant and product species were measured by a gas chromatograph (HP 7820), with separation using capillary column (Supelco, Carboxene-1006 PLOT, 30m x 0.53mm I.D.) and a thermal conductivity detector. Temperature programmed CO hydrogenation reaction was also performed using 5% CO, with the same protocols.

Catalytic activity changes by sintering were tested by time-on-stream measurements at 350°C up to 16 hrs on the 0.1% Ru/Al<sub>2</sub>O<sub>3</sub> catalyst prepared by the same pretreatments under the same reaction conditions as described previously. Steady state activities were measured at 280 ~ 320°C, which shown stable activities up to 1 h, with different Ru loaded catalysts using newly activated samples for each temperature and initial activities were extrapolated. Catalytic activities were evaluated under conditions where CO<sub>2</sub> conversion stayed below 5% . Turn-over-frequencies (TOF, number of CO<sub>2</sub> converted/Ru<sub>surface</sub>·s) were calculated based on the number of surface Ru atoms (as determined from H<sub>2</sub> chemisorption measurements) on alumina. For the H<sub>2</sub> chemisorption experiments the catalysts were pretreated under identical conditions that were applied prior to the catalytic tests. The amount of chemisorbed H<sub>2</sub> was determined on the thus treated samples using a Micromeritics AutoChem 2920 Chemisorption Analyzer apparatus. The

activated catalyst (calcined then reduced) was held at 100 °C during H<sub>2</sub> chemisorption measurements.

High-resolution TEM imaging was performed with a FEI Titan 80-300 microscope operated at 300 kV. The instrument is equipped with a CEOS GmbH double-hexapole aberration corrector for the probe-forming lens, which allows imaging with 0.1 nm resolution in scanning transmission electron microscopy (STEM) mode. The images were acquired in high angle annular dark field (HAADF) with an inner collection angle of 52 mrad. The sample preparation for the TEM measurements involved mounting of the powder samples on lacey carbon TEM grids, and immediate loading into the TEM airlock to minimize extended exposure to atmospheric O<sub>2</sub>.

## Results and Discussion

CO<sub>2</sub> conversion (panel a) and yields of CO (panel b) and CH<sub>4</sub> (panel c) obtained in the temperature programmed CO<sub>2</sub> reduction experiments on 0.1, 0.5, 1, 2 and 5 wt% Ru/Al<sub>2</sub>O<sub>3</sub> samples are displayed in Figure 1. On the 5% Ru/Al<sub>2</sub>O<sub>3</sub> catalyst, the CO<sub>2</sub> reduction starts at ~150 °C and shows the maximum conversion at ~320 °C and then the conversion decreases with further temperature increase to ~500 °C. Above 500 °C the CO<sub>2</sub> conversion increases again. With decreasing Ru loading the CO<sub>2</sub> conversion profiles are shifted toward higher temperature. On the 0.1 wt% Ru/Al<sub>2</sub>O<sub>3</sub> sample, CO<sub>2</sub> reduction starts above ~300°C and monotonically increases, then slows down above 450 °C. CO<sub>2</sub> conversion levels above this temperature (~450°C) are practically the same for all Ru loadings studied, although the loading changes by a factor of 50. Even though CO formation starts at practically the same temperature (~300°C) for all Ru-loaded samples, the activity profiles were very different. Interestingly, catalysts with lower amount of Ru showed significantly higher rate of CO formation at relatively low temperature, while over Ru/Al<sub>2</sub>O<sub>3</sub> catalysts with Ru loading  $\geq 2$  % the CO yield increased monotonically. The highest CO yield in the 350-500 °C temperature range was observed for the lowest Ru-loaded sample (0.1%). The CO yield increased rapidly after the onset temperature of ~350 °C, but then it leveled off between 450 and 500 °C, and at even higher temperatures it followed exactly the same path we observed for all the other catalysts. When the Ru loading increased to 0.5% the trend in the CO yield was similar to that observed for the 0.1% sample, however, its initial high activity leveled off at a much lower CO yield than that seen for the 0.1% catalyst. For the 1% sample the high CO yield region at low temperature is even less evident

than over the other two low Ru-loaded samples, but it is still clearly distinguishable. Above 500 °C the CO yield profiles are identical for all catalysts studied, and practically fall on a single line. The CH<sub>4</sub> yield profiles indicate that methane formation rate increases with increasing Ru loading and, at the same time, the temperature where the maximum methane yield is observed shifts to lower values with increasing Ru loading. These temperature programmed reaction results were completely consistent with our previously reported results on CO<sub>2</sub> reduction on Pd/alumina, where we have unambiguously showed that isolated, single Pd atoms favor the formation of CO, while methane formation is prevalent on Pd clusters. These results are very peculiar in light that Ru has been well known as a very efficient methanation catalyst [15]. The CO<sub>2</sub> conversion as well as the CO and CH<sub>4</sub> yields trends seem to suggest the existence of three different reaction regimes as the temperature is increased from 25 to 500 °C. The formation of CH<sub>4</sub> is prevalent at low reaction temperatures, and the CH<sub>4</sub> yield increases proportionally with Ru loading. This is in line with the conclusions of earlier studies that CH<sub>4</sub> formation is favored on large metal clusters. With increasing Ru loading the size of metal clusters increases, as it has been substantiated by TEM measurements. At very low Ru loading (0.1 wt%) (highly dispersed Ru) no CH<sub>4</sub> formation is seen even at temperatures (~350 °C) where the CH<sub>4</sub> yield reached its maximum at high Ru loadings. As we will show in the following paragraph, the low Ru-loaded catalyst exhibits CH<sub>4</sub> formation activity only after the onset of metal sintering, i.e., after the formation of 3D metal clusters. The maximum in the CO<sub>2</sub> conversion vs. temperature plot can solely be attributed to the maximum in CH<sub>4</sub> formation rate. This behavior suggests that at high temperature the concentration of one of the reactants (either CO<sub>2</sub> or H<sub>2</sub>) on the catalyst surface decreases which leads to a drop in CO<sub>2</sub> conversion, and also in the CH<sub>4</sub> yield. In the second temperature regime the dominant reaction is the formation of CO on highly dispersed Ru particles. At low Ru loadings we see a particular shape of the CO yield traces as a function of temperature. The onset temperature of CO formation at low Ru loadings is around 320 °C. At the lowest Ru loading (0.1 wt%) the CO yield increases fast with temperature, levels off around 450 °C and then increases again above 500 °C. With increasing Ru loading, however, the CO yield drops, and over the 5 wt% Ru-loaded sample we observe no CO formation. CO is only produced on this sample as a result of a secondary reaction at this high temperature between CH<sub>4</sub> formed on Ru clusters and the reactant CO<sub>2</sub> (dry reforming of CO<sub>2</sub>). (The observed increase in CO yield above 500 °C over the low Ru loaded samples can also be attributed to the onset of this

secondary reaction.) The increase in CO<sub>2</sub> conversion at high temperatures (above 500 °C) on all samples studied here can be attributed to the reaction between CH<sub>4</sub> and CO<sub>2</sub>.

CO<sub>x</sub> methanation over supported Ru catalysts has been shown to be structure sensitive as it depended on the particle size of Ru clusters [16-21]. For CO hydrogenation Che et al. [21] observed that the TOF decreased with increasing Ru dispersion, and similar findings for CO<sub>2</sub> methanation was reported by Kowalczyk et al [16] (although, in the latter study the size of Ru clusters was shown to affect the CO<sub>2</sub> hydrogenation rate in a lesser extent than the CO hydrogenation). The variation in the methanation rate with Ru particle size might be (at least in part) correlated with the effect of the support on the metal particles. The electronic state (charge density) of the Ru particles on a given support material (here Al<sub>2</sub>O<sub>3</sub>) may vary with particle size, as it was proposed by Scire et al. [22], who reported that the electronic state of the active metal (Ru) strongly influenced the CO selectivity in the CO<sub>2</sub> hydrogenation process. They proposed that a more oxidized Ru surface led to higher methanation activity, due to the higher hydrogen and lower CO coverage. In order to vary the electronic properties of Ru particles supported on YSZ solid electrolyte pellets Theleritis et al. [23] used the electrochemical promotion of catalysis (EPOC) effect by applying external potential to the catalytic system. They found that at low temperatures (up to 240 °C) CO<sub>2</sub> hydrogenation reaction yielded CH<sub>4</sub> primarily, while CO was the dominant product at high temperatures. Electrochemical O<sup>2-</sup> supply to the Ru particles resulted in large increases in both the formation rate and selectivity of CH<sub>4</sub>, and concomitantly a large decrease in the CO formation rate.

The results of these temperature programmed reaction measurements may also be argued on the basis of having more Ru in the catalyst translates to higher hydrogenation activity and, therefore, extensive CH<sub>4</sub> formation. This interpretation, however, cannot explain the formation of larger amount of CO on catalysts containing less amount of Ru. In order to address this issue, we performed isothermal CO<sub>2</sub> hydrogenation on the 0.1% Ru/Al<sub>2</sub>O<sub>3</sub> catalyst at 350 °C. At this temperature single Ru atoms present on the alumina support initially show sintering during the course of reaction. The initial selectivity of CO formation at this catalyst bed temperature is much higher (over 84%) than that of CH<sub>4</sub> production on the 0.1% Ru/Al<sub>2</sub>O<sub>3</sub> catalyst, as shown in Figure 2(a). With increasing time-on-stream, CO production rate increased slowly, while the CH<sub>4</sub> formation rate increased much faster and after ~ 200 min time-on-stream, CO and CH<sub>4</sub> were produced in almost the same amounts. After 16 hrs time-on-stream, CH<sub>4</sub> production far

exceeded the formation of CO, as the CO selectivity dropped to ~36%. These results indicate that the Ru/Al<sub>2</sub>O<sub>3</sub> catalysts with low Ru loadings are not stable under the reducing reaction conditions of CO<sub>2</sub> reduction. In order to compare the activities of fresh and used catalysts, we evaluated the steady state activities of two 0.1% Ru/Al<sub>2</sub>O<sub>3</sub> catalysts at 300 °C: a freshly prepared catalyst and the one that was reactivity tested at 350 °C for 16hrs. The fresh catalyst showed stable steady state activity at this lower reaction temperature of 300 °C in comparison to that observed at 350 °C. As the results of Figure 2(b) substantiate, the overall CO<sub>2</sub> conversion activity of the 350 °C-tested catalyst increased ~ 4.5 times and most of the activity increase came from the ~ 20 fold increase in the CH<sub>4</sub> production rate. At the same time, the increase in CO TOF at steady state at 300 °C over the 350 °C-tested sample was much smaller, only about 1.5X. A likely explanation for the observed variation in catalytic activity at high temperature with time-on-stream is the change in metal particle size under reaction conditions. As we have seen for the Pd/Al<sub>2</sub>O<sub>3</sub> catalysts [11] both the overall catalytic activity (i.e., CO<sub>2</sub> conversion) and the product (CO and CH<sub>4</sub>) selectivity were strongly dependent on the active metal particle size. In order to visualize the change in metal particle size (changes in Ru dispersion), we collected STEM images from two catalyst samples: from a freshly prepared 0.1% Ru/Al<sub>2</sub>O<sub>3</sub> catalyst and from the one that was reaction-tested at 350 °C. The freshly prepared 0.1% Ru/Al<sub>2</sub>O<sub>3</sub> sample showed almost exclusively atomically dispersed Ru (and very small Ru aggregates) on the alumina support (image a in Fig. 3). On the contrary, after reaction test at 350 °C for 16 hrs, mostly nm-sized (some of them even larger than 5 nm) 3D Ru clusters are visible in the STEM images (image c in Fig.3). These results strongly support our hypothesis that CO formation is favored on single Ru atoms supported on alumina, while Ru clusters are mostly active for CH<sub>4</sub> formations. Therefore, we conclude that the high methanation activity reported for Ru on alumina catalysts originate from large (3D) Ru clusters. The catalytic data discussed in the previous section seem to suggest that the reaction mechanism is different for the small (atomically dispersed) and larger (3D) Ru particles. Therefore, next we investigated how the reaction mechanisms changed with the variation of active metal particle size. To this end, we performed kinetic measurements on all the Ru-loaded alumina supported catalysts prepared (from 0.1 to 5% Ru loading). A series of Arrhenius plots of CO<sub>2</sub> TOF (calculated based on the number of surface Ru atoms on the alumina supported metal clusters) are displayed in Fig. 4(a), each showing reasonably linearity in temperature regime explored in this study (270-350 °C).



The CO<sub>2</sub> TOF is the lowest over the 0.1wt% Ru/alumina catalyst, and increases dramatically over the 0.5 wt% sample, and further over the 1 wt% catalyst. Above 1 wt% Ru loading the CO<sub>2</sub> TOF increases only marginally.. Good linearity in the Arrhenius plots for both CO and methane TOFs is shown in Figure 4(b) and (c), respectively, except for the 0.1% Ru/Al<sub>2</sub>O<sub>3</sub> sample which is related to the significant error in the calculation of TOF due to low CH<sub>4</sub> selectivity. At Ru loadings up to 2 % the CO TOF values are very similar, and only drop significantly on the highest Ru loaded sample (5 wt%), as large metal clusters tend to produce no CO. The TOF plots of CH<sub>4</sub> at Ru loadings higher than 1% are very close to each other, but there is a systematic increase in CH<sub>4</sub> TOF with increasing Ru loading. This observation suggests that Ru clusters exhibit very similar catalytic activities toward CH<sub>4</sub> formation above a certain cluster size. These results are consistent with our previous interpretations that single Ru atoms or interfacial Ru favor CO formation, while Ru clusters favor CH<sub>4</sub> formation. From the slopes we can estimate the apparent activation energies of CO and CH<sub>4</sub> formation. Interestingly, the activation energy for CO formation (~82 kJ/mol) was always ~20 kJ/mole higher than that for CH<sub>4</sub> formation (~62 kJ/mol), regardless of Ru loading. If one considers CO as an intermediate in the path toward CH<sub>4</sub> formation in the CO<sub>2</sub> hydrogenation process, the activation energy for CO formation should be equal to or lower than that for CH<sub>4</sub> formation. Therefore, we propose that CO is either formed by a different route (not as an intermediate in the reduction toward CH<sub>4</sub>) or on a different active center than CH<sub>4</sub>. The E<sub>a</sub> for methane formation obtained from the Arrhenius plots in this study is comparable to those reported previously by Solymosi et al. [24,25] for CO<sub>2</sub> methanation over 5% Ru/Al<sub>2</sub>O<sub>3</sub> (67.4 kJ/mol), and by Bartholomew et al. [26] for Ru/SiO<sub>2</sub> (72 kJ/mol). Changes in the apparent activation energy with reaction conditions applied has also been reported in the latter publication, due, possibly, to the variation in the rate determining step under different reaction conditions.

In Figure 5(a), we show CO and CH<sub>4</sub> TOFs measured at 300 °C as a function of Ru loading in the reduction of CO<sub>2</sub>. With increasing Ru loading the trends in CO and CH<sub>4</sub> TOFs are opposite: the TOF for CO formation is practically constant up to 2 wt% Ru loading and then it decreases, while that for CH<sub>4</sub> formation increased in the entire Ru loading regime studied (0.1 – 5 wt%). The CO selectivity below 1% Ru on alumina is evidently increases sharply with the decrease in Ru loading (Fig. 5b). We believe that these results indicate high Ru dispersion at loadings less than 1%, when most of the Ru is present as isolated single atoms and small metal aggregates, and

the production of CO is favored. On the other hand, at Ru loadings high enough to form Ru clusters (starting from ~1%), the reduction of CO<sub>2</sub> proceeds all the way to CH<sub>4</sub>. These results are fully consistent with our previous report on the reactivity of isolated Pd atoms that have been shown to favor the formation of CO, while mostly CH<sub>4</sub> formed on the Pd clusters [11]. The results of both of these studies strongly suggest that the active sites for CO formation are highly dispersed single metal atoms (these form CO with high selectivity), and possibly small metal aggregates, as well. However, the formation of CH<sub>4</sub> can only proceed in the presence of metal clusters that are able to supply large amounts of atomic hydrogen to this process. As we have mentioned above, the apparent activation energy for CH<sub>4</sub> formation is about 20 kJ/mol lower than that of CO formation over every Ru/Al<sub>2</sub>O<sub>3</sub> catalyst studied here. This result seems to suggest that CH<sub>4</sub> production may not proceed through an intermediate that formed from CO produced in the initial reduction step. To test this we performed temperature programmed reduction of both CO and CO<sub>2</sub> on freshly prepared 0.1% Ru/Al<sub>2</sub>O<sub>3</sub> catalysts. As the results displayed in Figure 6 show, the onset temperature for CO<sub>2</sub> hydrogenation on the 0.1% Ru/Al<sub>2</sub>O<sub>3</sub> is ~300-350 °C, while that for CO hydrogenation is ~500 °C. We propose that this ~150 °C upward shift in the on-set temperature for hydrogenation provides two important insights into the reaction mechanisms. First, CO<sub>2</sub> hydrogenation to CO might proceed by two different, in parallel occurring mechanisms: hydrogenation on metallic surfaces and reverse water gas shift reaction. Second, alumina supported isolated single Ru atoms can catalyze CO<sub>2</sub> reduction to CO but cannot catalyze further hydrogenation to CH<sub>4</sub> due, perhaps, to their limited hydrogen activation functionality. This would be consistent with our previous finding [11] in that dual catalyst functionality was required for CO<sub>2</sub> hydrogenation to CH<sub>4</sub> over supported Pd catalysts. In a Ru-doped ceria catalyst Metiu et al., [27] have also found that “gas-phase CO is not a reaction intermediate for the methanation of CO<sub>2</sub> by Ce<sub>0.95</sub>Ru<sub>0.05</sub>O<sub>2</sub>”. In a recent study Ussa Aldana et al. carried out *in operando* FTIR measurements on the CO<sub>2</sub> methanation reaction over Ni/CeZrO<sub>2</sub> catalysts [28]. Their results unambiguously show that methane formation does not go through a CO intermediate, rather surface carbonate/formate species formed on the oxide support play a critical role in the formation of CH<sub>4</sub>. Adsorbed CO<sub>2</sub> is proposed to hydrogenate stepwise, forming bicarbonates, formates, formaldehyde, and finally methoxide. Supported Ni clusters dissociate H<sub>2</sub> and supply H atoms for these hydrogenation steps. The mechanism of CO<sub>2</sub> methanation on supported Ru catalysts has also been strongly debated, and no clear consensus on

the actual reaction path has been reached. Based on the results of a DRIFT spectroscopy study Prairie et al. proposed formic acid as a critical intermediate in the CO<sub>2</sub> methanation process [29]. Subsequently, the role of formic acid or formate intermediate was questioned by Traa et al., who found in their kinetic study on CO<sub>2</sub> methanation over Ru/TiO<sub>2</sub> catalysts that CH<sub>4</sub> formation proceeded through the hydrogenation of surface carbon as the rate determining step [30]. Our current kinetic and spectroscopy studies are focused on understanding the reaction mechanisms for the formation of both CO and CH<sub>4</sub> over these Ru-based catalysts at different Ru loadings, and identifying active catalytic centers of these materials and key reaction intermediates.

### Conclusion:

The reactivities of Ru/Al<sub>2</sub>O<sub>3</sub> catalysts in the Ru loading range of 0.1-5wt% were studied in the reduction of CO<sub>2</sub> with H<sub>2</sub>. The main focus of the work was to find correlation between the active metal dispersion and the catalytic performance of these materials. At very high metal dispersion (metals mostly present in atomic dispersion, as evidenced by STEM) the catalyst produces CO with high selectivity. As 3D metal clusters form at higher Ru loadings (at and above 1 wt%) or as a result of sintering, the selectivity toward CH<sub>4</sub> formation increases significantly. Catalysts with low metal loading, however, are unstable under reaction conditions of CO<sub>2</sub> reduction, and form large metal clusters. This clustering is accompanied by a large increase in CH<sub>4</sub> selectivity and drop in CO formation selectivity. Apparent activation energies of 82 and 62 kJ/mol were estimated from the slopes of Arrhenius plots for CO and CH<sub>4</sub> formation, respectively. The difference in activation energy of ~20 kJ/mol for each catalyst studied suggests either different reaction paths for the formation of CO and CH<sub>4</sub>, or/(and) different active sites. The higher apparent activation energy for CO formation also seems to suggest that CO is not an intermediate in the formation of CH<sub>4</sub>. This is further supported by the results of activity measurements over a 0.1% Ru/Al<sub>2</sub>O<sub>3</sub> catalyst, that showed about 125 °C onset temperature difference between the CO<sub>2</sub> (~325 °C) and CO (~450 °C) reduction.

### Acknowledgements

We thank Dr. Feng Gao for carrying out the H<sub>2</sub> chemisorption measurements on all the Ru/Al<sub>2</sub>O<sub>3</sub> catalysts discussed in this work. The catalyst preparation and catalytic measurements were supported by a Laboratory Directed Research and Development (LDRD) project, while the TEM work was supported by the Chemical Imaging Initiative at the Pacific Northwest National

Laboratory (PNNL). PNNL is operated for the US Department of Energy by Battelle Memorial Institute under contract number DE-AC05-76RL01830. JHK also acknowledges the support of this work by the 2013 Research Fund of UNIST (Ulsan National Institute of Science and Technology, Ulsan, Korea).

## References:

1. Boffa, A.; Lin, C.; Bell, A.T.; Somorjai, G.A., *J.Catal.*, **1994**, *149*, 149.
2. Wambach, J.; Baiker, A.; Wokaun, A. *Phys.Chem.Chem.Phys.*, **1999**, *1*, 5071.
3. R.P.A. Sneed, *J.Mol.Catal.*, **1982**, *17*, 349.
4. Fisher, I.A.; Bell, A. T. *J.Catal.*, **1996**, *162*, 54.
5. Baiker, A. *Appl.Organomet.Chem.*, **2000**, *14*, 751.
6. Peterson, A. A.; Abild-Pedersen, F.; Studt, F.; Rossmeisl, J.; Norskov, J.K. *Energy & Environ.Sci.*, **2010**, *3*, 1311.
7. Durand, W.J.; Peterson, A.A.; Studt, F.; Abild-Pedersen, F.; Norskov, J.K. *Surf.Sci.*, **2011**, *605*, 1354.
8. Ferrin, P.; Mavrikakis, M. *J.Am.Chem.Soc.*, **2009**, *131*, 14381.
9. Clarke, D. B.; Bell, A.T.; *J.Catal.*, **1995**, *154*, 314.
10. Clarke, D.B.; Suzuki, I.; Bell, A.T.; *J.Catal.*, **1993**, *142*, 27.
11. Kwak, J.H.; Kovarik, L.; Szanyi, J. *ACS Catalysis*, *in press*, DOI: 10.1021/cs4001392.
12. Solymosi, F.; Erdöhelyi, A.; Kocsis, M.; *J.Chem.Soc.-Faraday Trans.*, **1981**, *77* 1003.
13. Elliott, D.J.; Lunsford, J.H.; *J.Catal.*, **1979**, *57* 11.
14. Kusmierz, M.; *Catal. Today*, **2008**, *137* 429.
15. Mills, G.A.; Steffgen, F.W. *Catal. Rev.*, **1973**, *8* 159.
16. Kowalczyk Z., Stolecki, K., Rarog-Pilecka, W., Moskiewicz, E., Wilczkowska, E., Karpinsky, Z., *Appl.Catal A: General*, **2008**, *342*, 35.
17. King, D.L., *J.Catal.*, **1978**, *51*, 386.
18. Kellner, S.C., Bell, A.T., *J.Catal.*, **1982**, *75*, 251.
19. Guzzi L., Schay, Z., Matusek, K., Bogyai, I., *Appl.Catal.*, **1986**, *22*, 289.
20. Venter, J.J., Vannice, M.A., *Inorg.Chem.*, **1989**, *28*, 1634.
21. Che M., Bennett C.O., *Adv.Catal.*, **1989**, *36*, 55.

22. Scire, S., Crisafulli, C., Maggiore, R., Minico, S., Galvagno, S., *Catal.Lett.*, **1998**, *51*, 41.
23. Theleritis, D., Souentie, S., Siokou, A., Katsaounis, A., Vayenas, C.G., *ACS Catal.*, **2012**, *2*, 770.
24. Solymosi, F. and Erdőhelyi, A. *J. Mol. Catal.*, **1980**, *8*, 471.
25. Solymosi F., Erdőhelyi, A., Bánsági, T. *J. Catal.*, **1981**, *68*, 371.
26. Weatherbee G.D.; Bartholomew, C.H. *J.Catal.* **1984**, *87*, 352-362.
27. Sharma, S.; Hu, Z.; Zhang, P.; McFarland, E.W.; H. Metiu *J.Catal.* **2011**, *278* 297.
28. Ussa Aldana, P.A.; Ocampo, F.; Kolb, K.; Louis B.; Thibault-Starzyk, F.; Daturi, M.; Bazin, P.; Thomas, S.; Roger, A.C. *Catal.Today*, DOI: 10.1016/j.cattod.2013.02.019.
29. Prairie, M.R., Renken, A., Highfield, J.G., Thampi, K.R., Grätzel, M., *J.Catal.*, **1991**, *129*, 130.
30. Traa, Y., Weitkamp, J., *Chem.Eng.Technol.*, **1999**, *21*, 4.

**Figure captions**

**Figure 1.** Temperature programmed CO<sub>2</sub> reduction reaction on Ru/Al<sub>2</sub>O<sub>3</sub> catalysts: CO<sub>2</sub> conversion (a), CO (b) and CH<sub>4</sub>(c) yields . ( $m_{\text{catalyst}}= 50 \text{ mg}$ , 5% CO<sub>2</sub> +15% H<sub>2</sub> in He (total flow rate = 60 ml/min), heating rate = 5 °C/min)

**Figure 2.** (a) TOFs of CO<sub>2</sub>, CO and CH<sub>4</sub> as a function of time-on-stream at 350 °C over a 0.1% Ru/Al<sub>2</sub>O<sub>3</sub> catalyst. (b) steady-state TOFs for CO<sub>2</sub> conversion and CO/CH<sub>4</sub> production over a fresh and re-activated (after reaction at 350 °C) 0.1% Ru/Al<sub>2</sub>O<sub>3</sub> catalyst at 300 °C.

**Figure 3.** STEM images from a 0.1% Ru/Al<sub>2</sub>O<sub>3</sub> catalyst before (images a and b) and after (images c and d) CO<sub>2</sub> reduction at 350 °C for 16 hrs.

**Figure 4.** Arrhenius plots for CO<sub>2</sub> conversion (a), as well as for CO (b) and CH<sub>4</sub> (c) formations over Ru/Al<sub>2</sub>O<sub>3</sub> catalysts between 270 °C and 350 °C.

**Figure 5.** (a) TOFs of CO and CH<sub>4</sub> formation at steady-state at 300 °C over Ru/Al<sub>2</sub>O<sub>3</sub> catalysts as a function of Ru loading (open symbols: data obtained from a 0.1% Ru/Al<sub>2</sub>O<sub>3</sub> catalyst that was tested previously at 350 °C). (b) CO selectivity as a function of Ru loading at 300 °C.

**Figure 6.** Temperature programmed CO and CO<sub>2</sub> conversions over a 0.1 % Ru/Al<sub>2</sub>O<sub>3</sub> catalyst.

**Figure 1(a).**

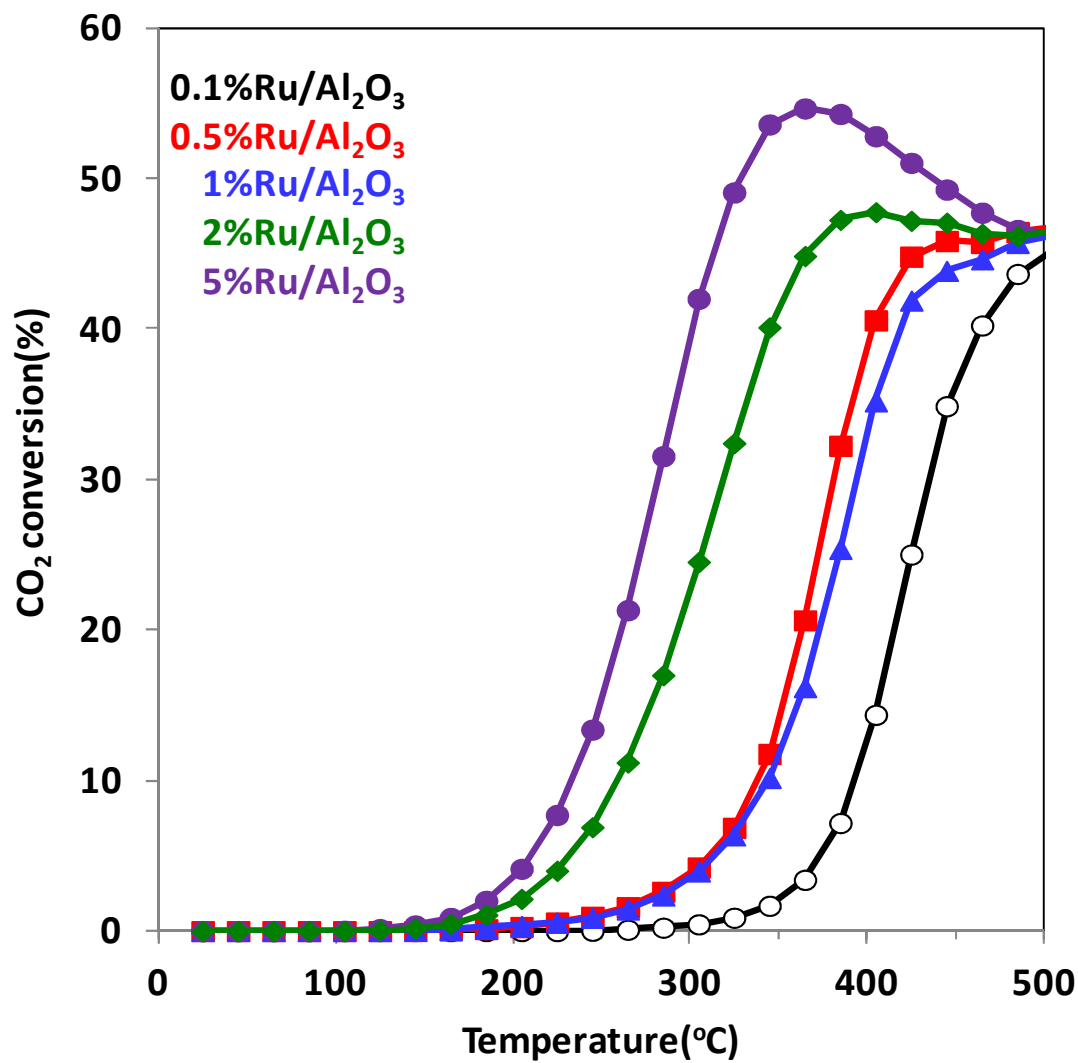


Figure 1(b)

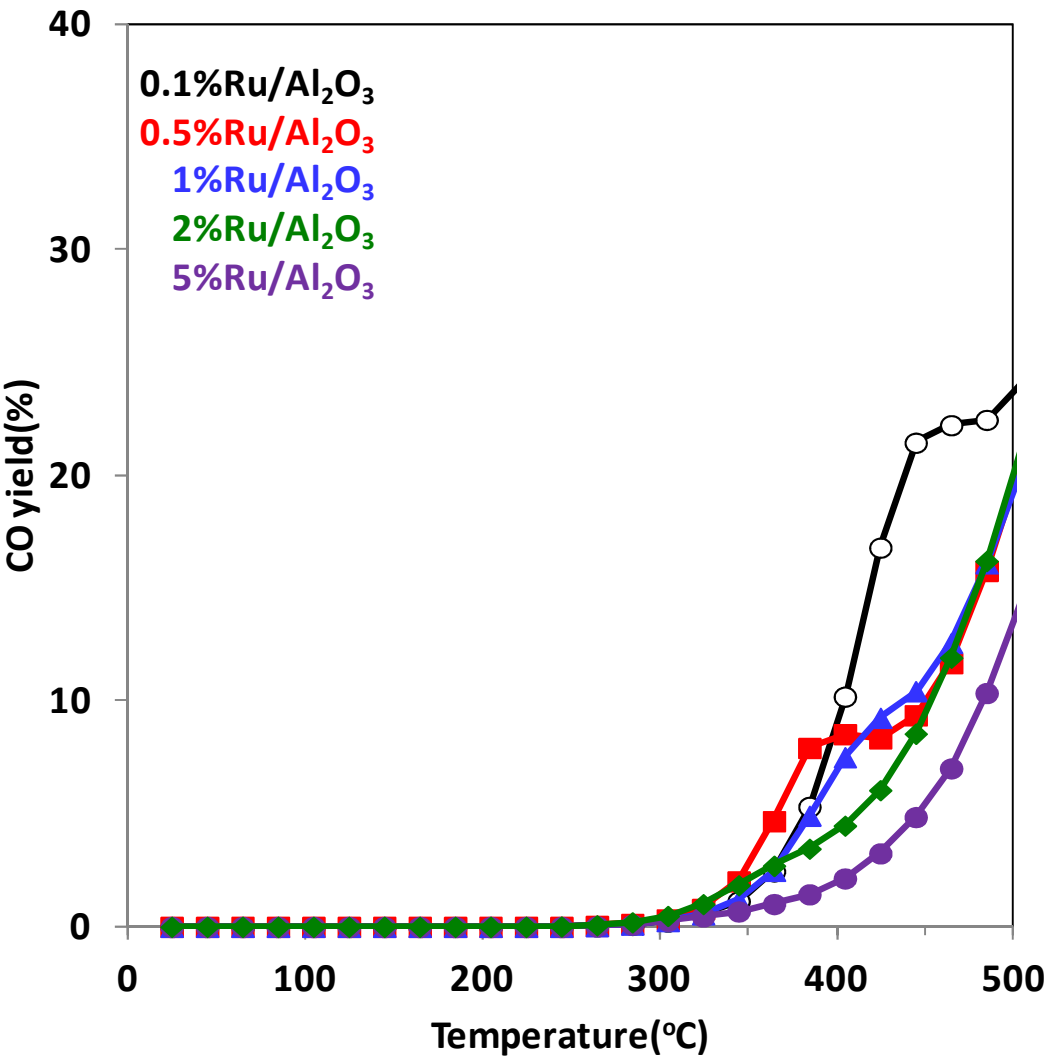




Figure 1(c)

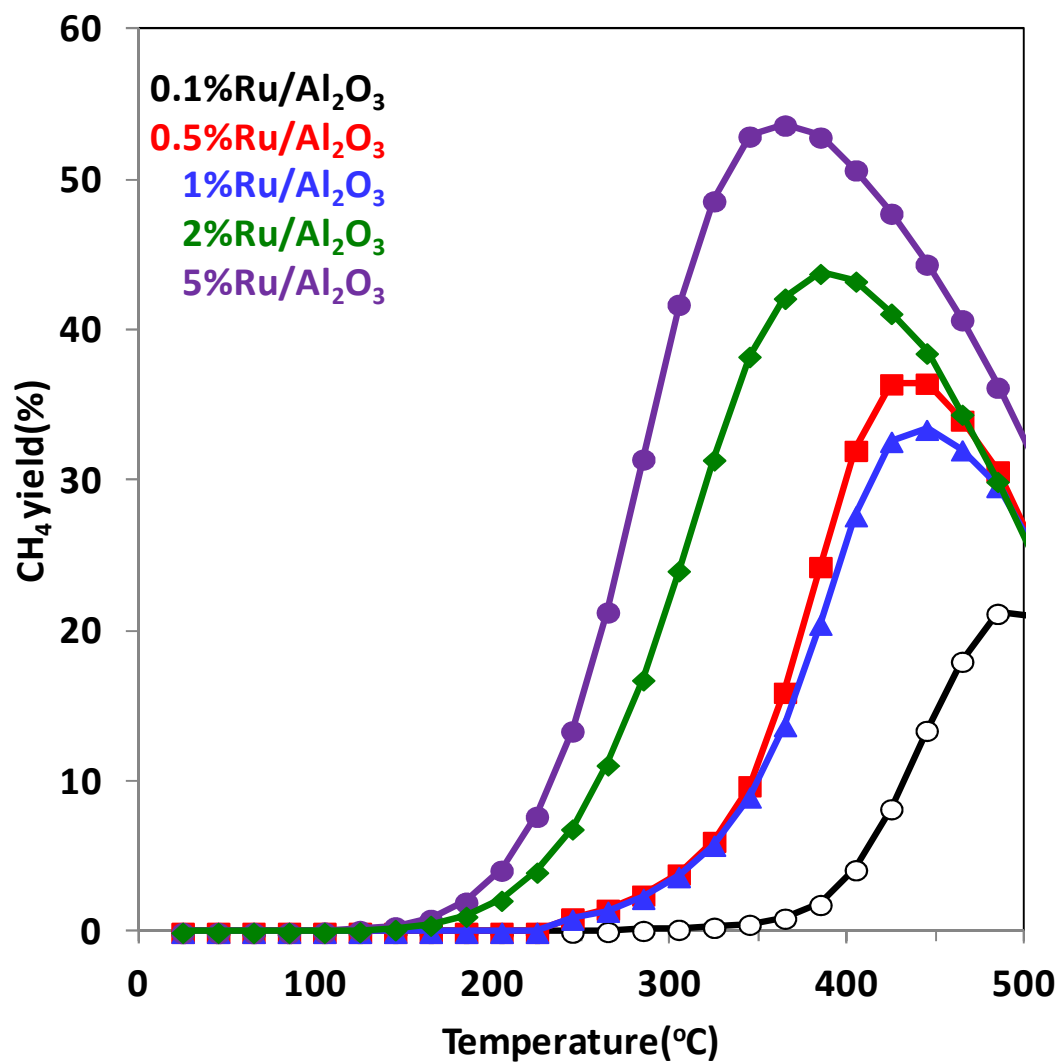


Figure 2(a)

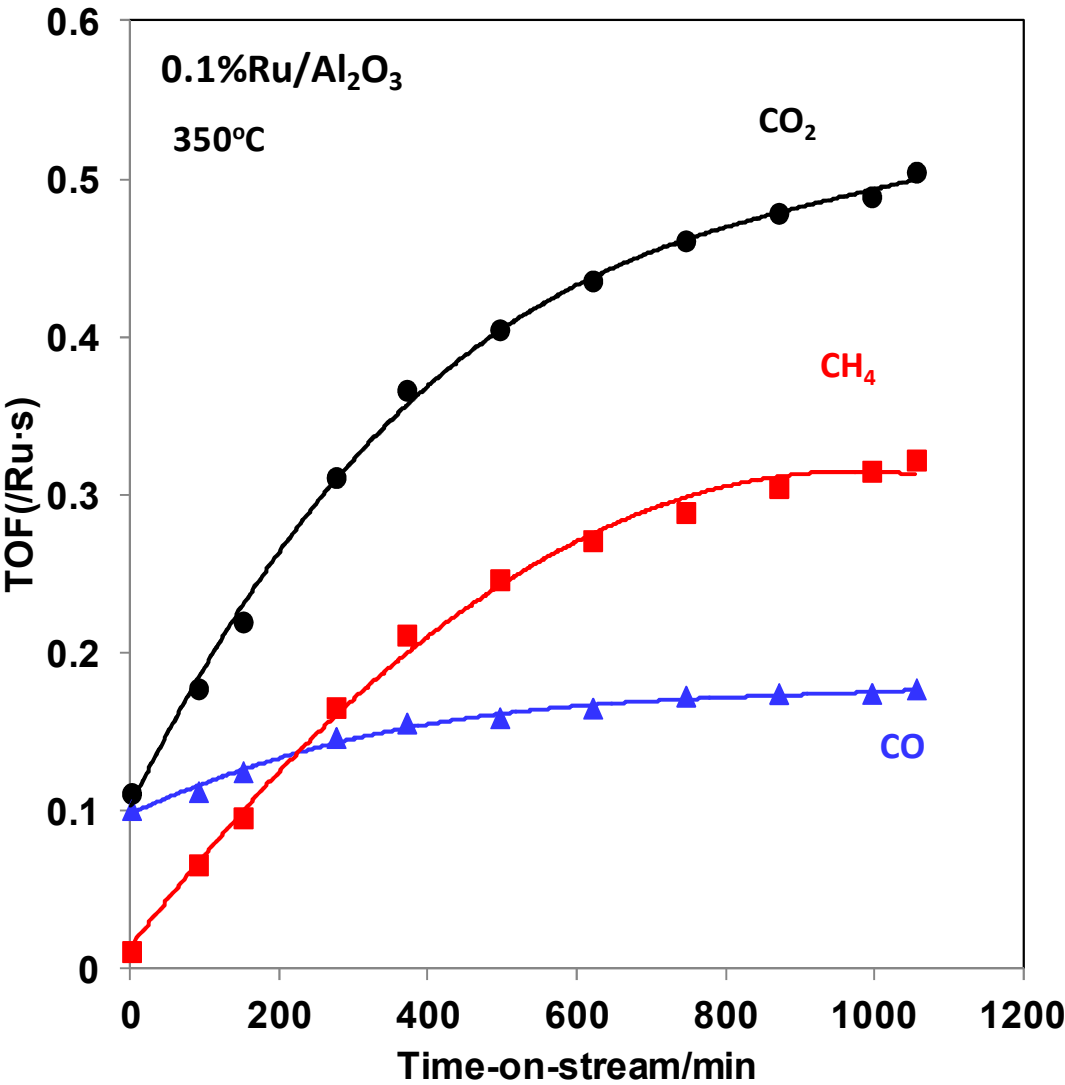


Figure 2 (b)

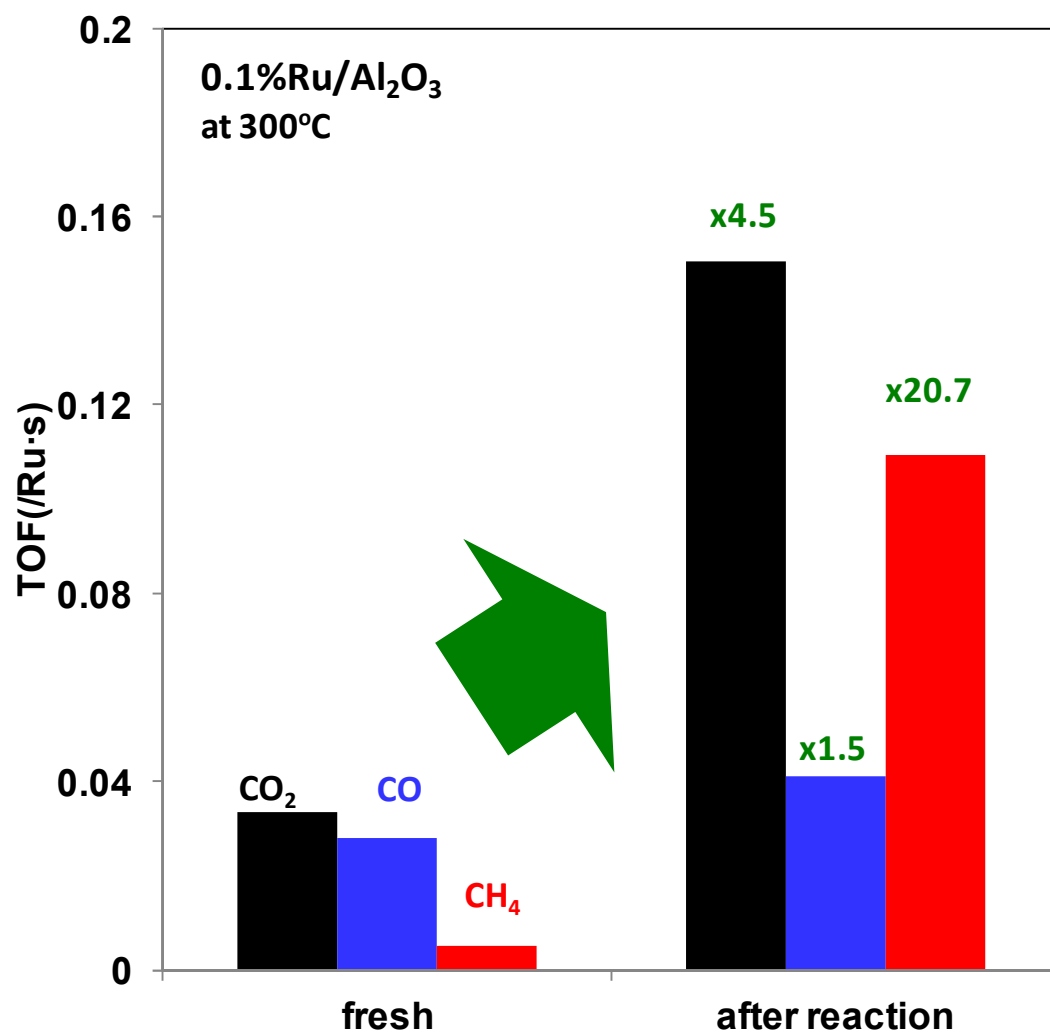


Figure 3.

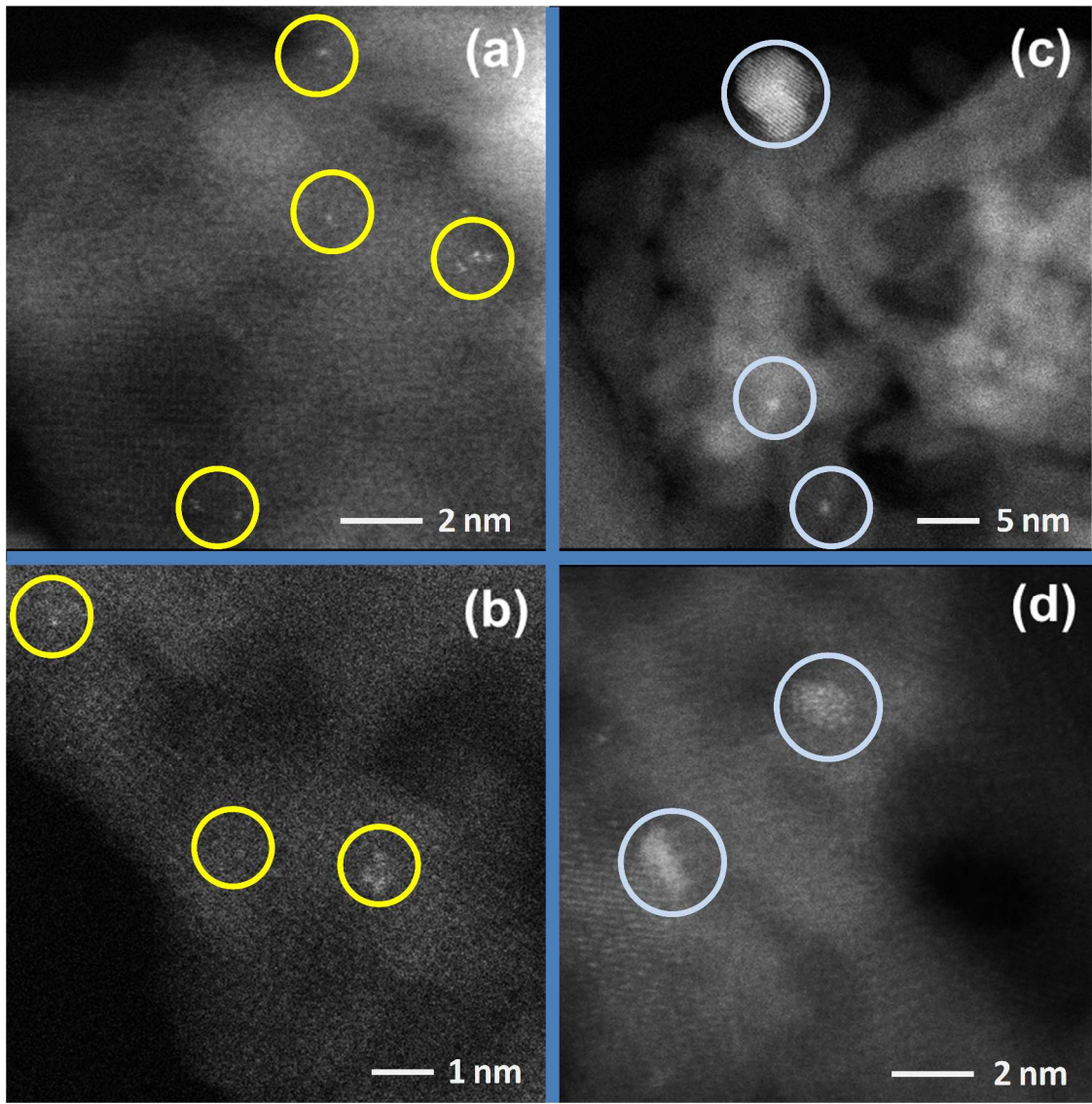


Figure 4(a)

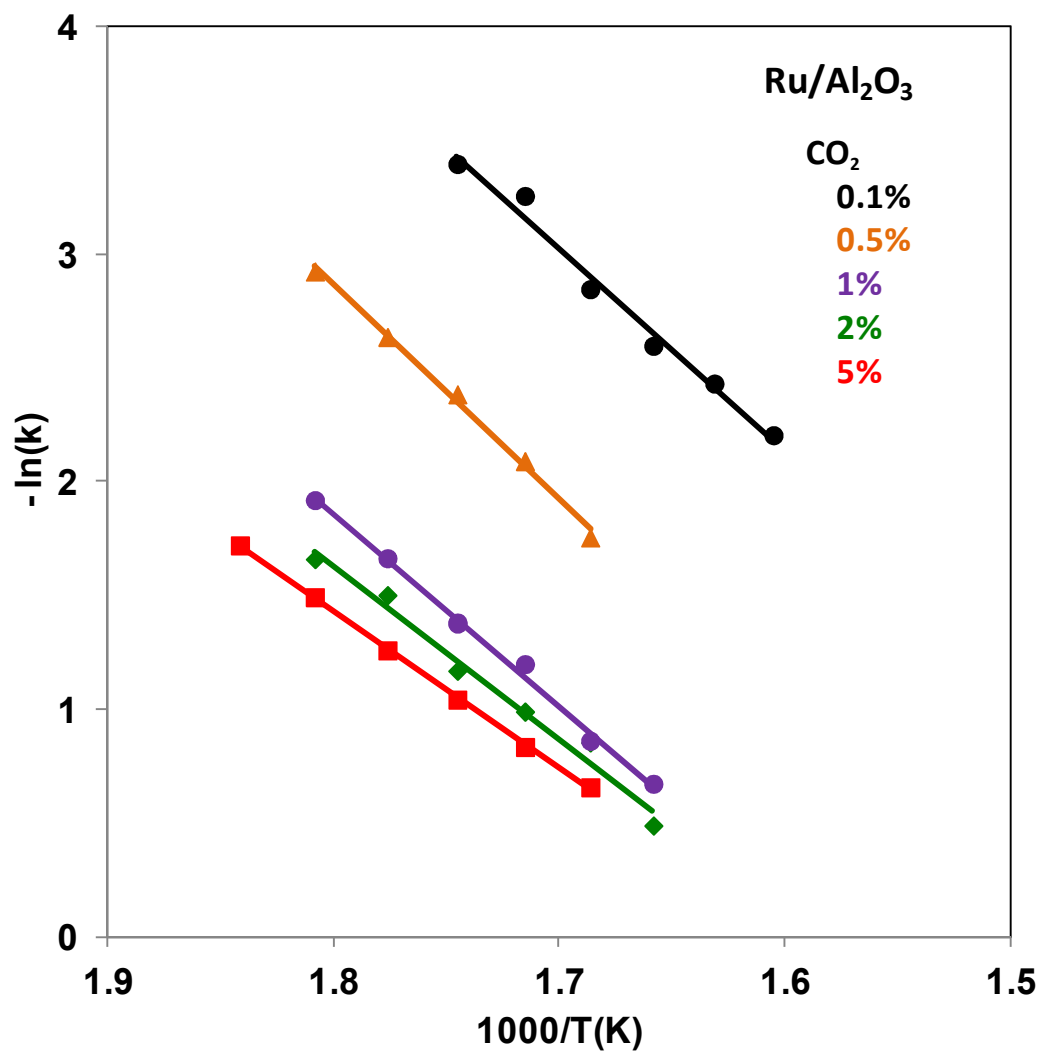


Figure 4(b).

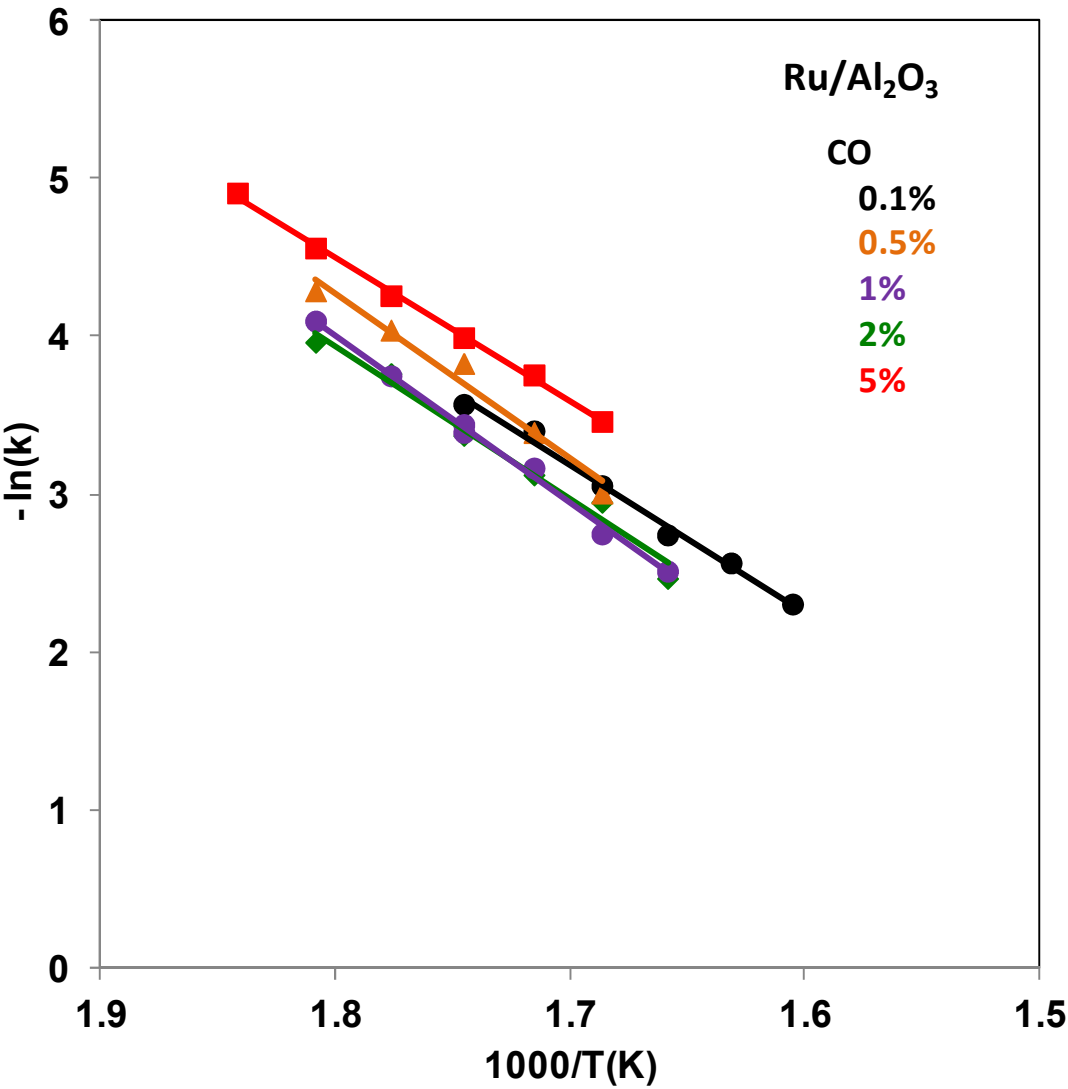


Figure 4(c)

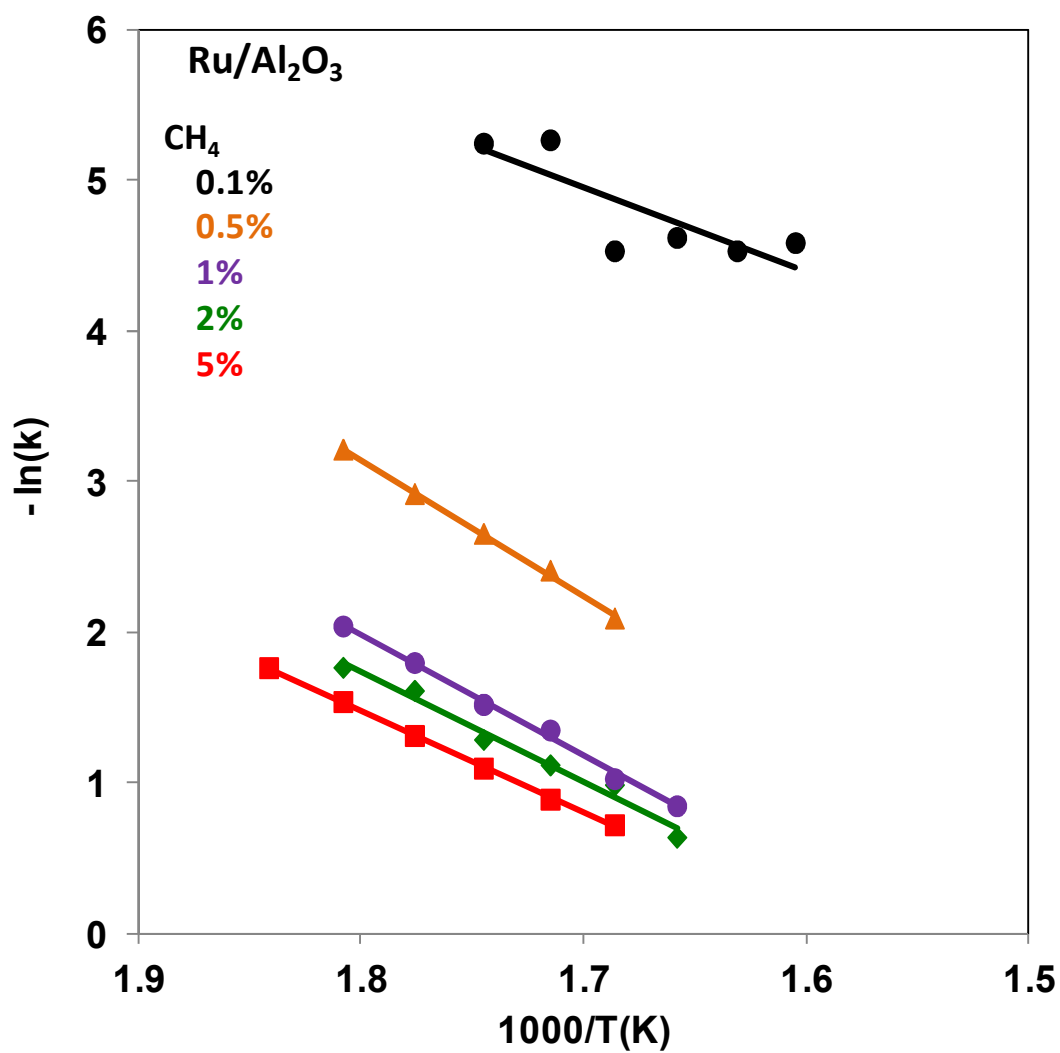


Figure 5(a)

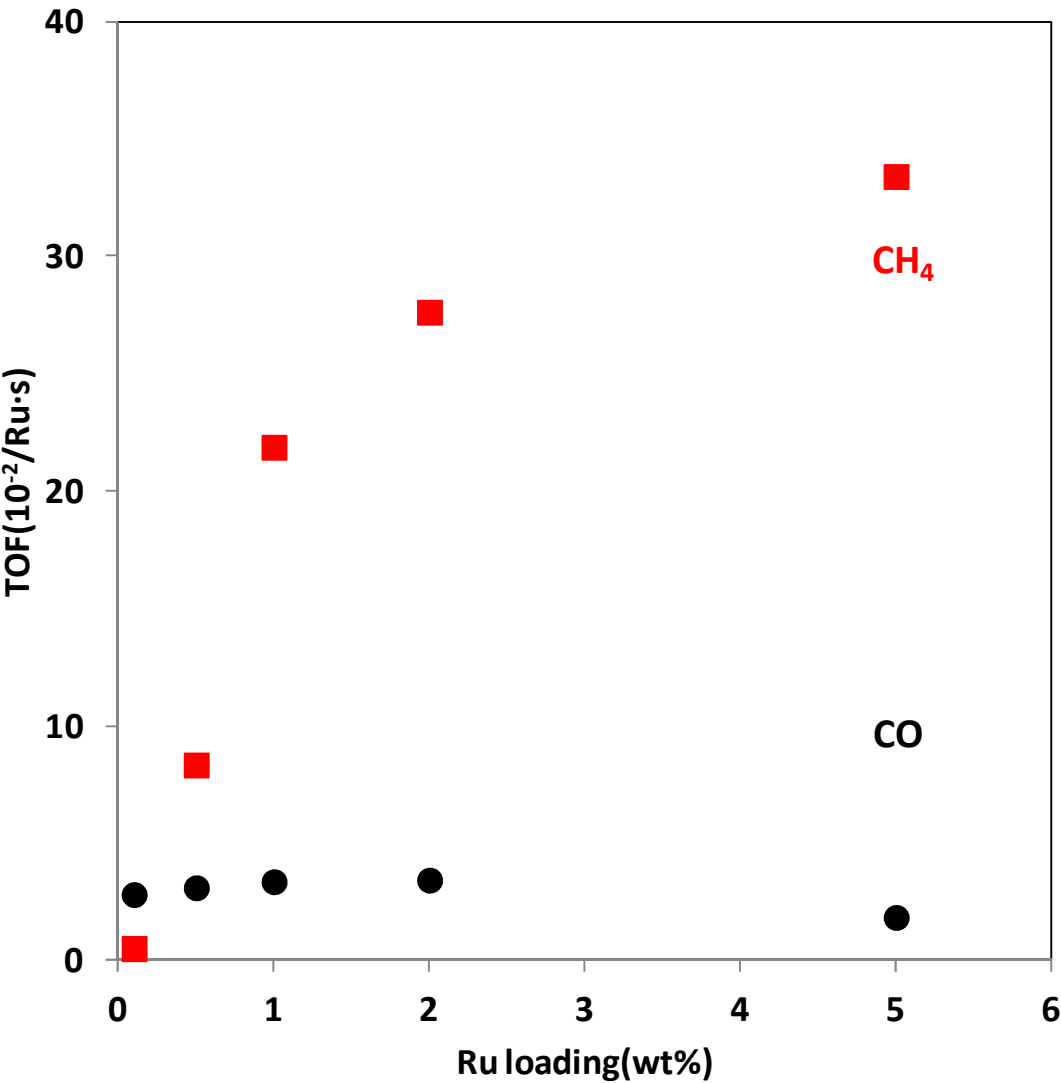




Figure 5(b)

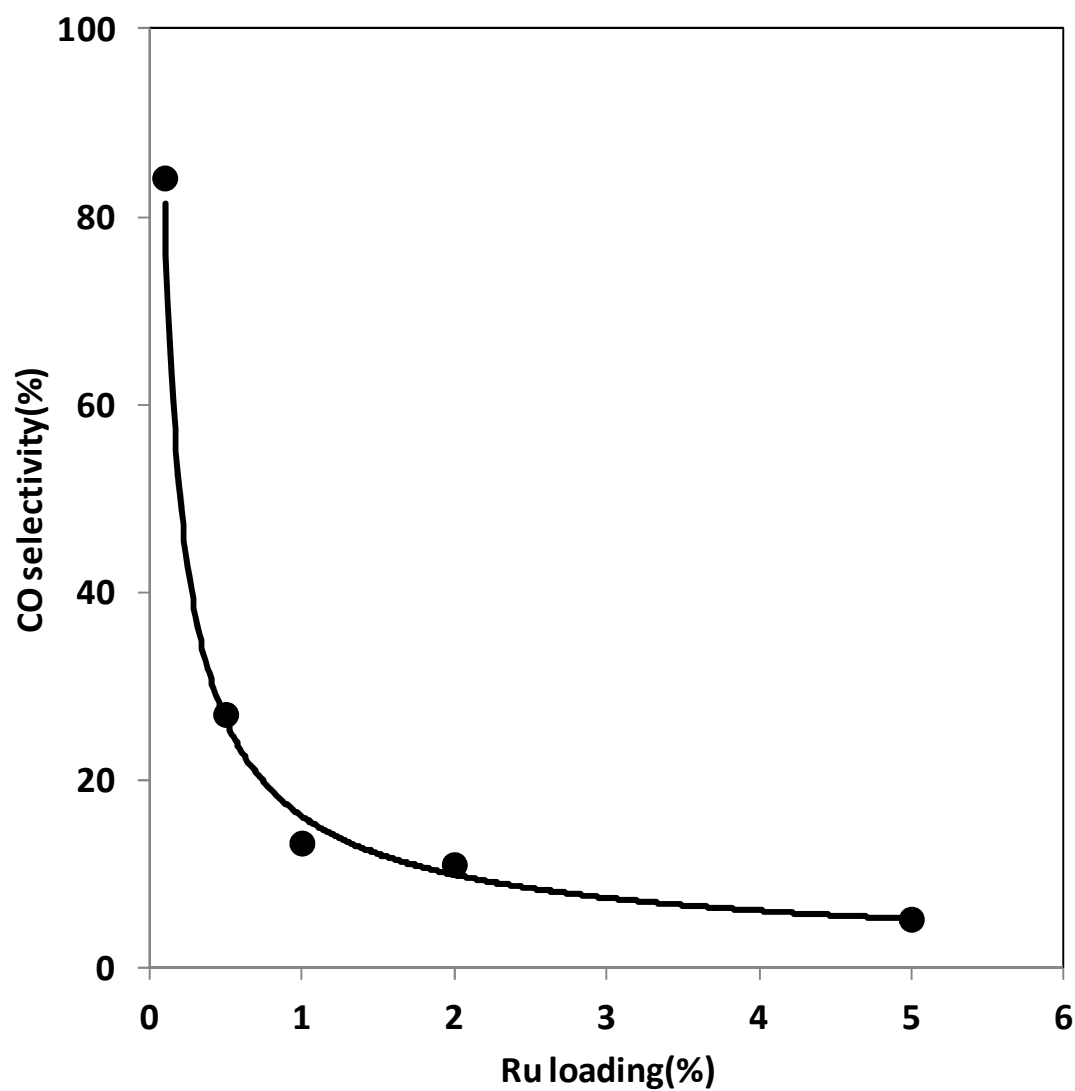
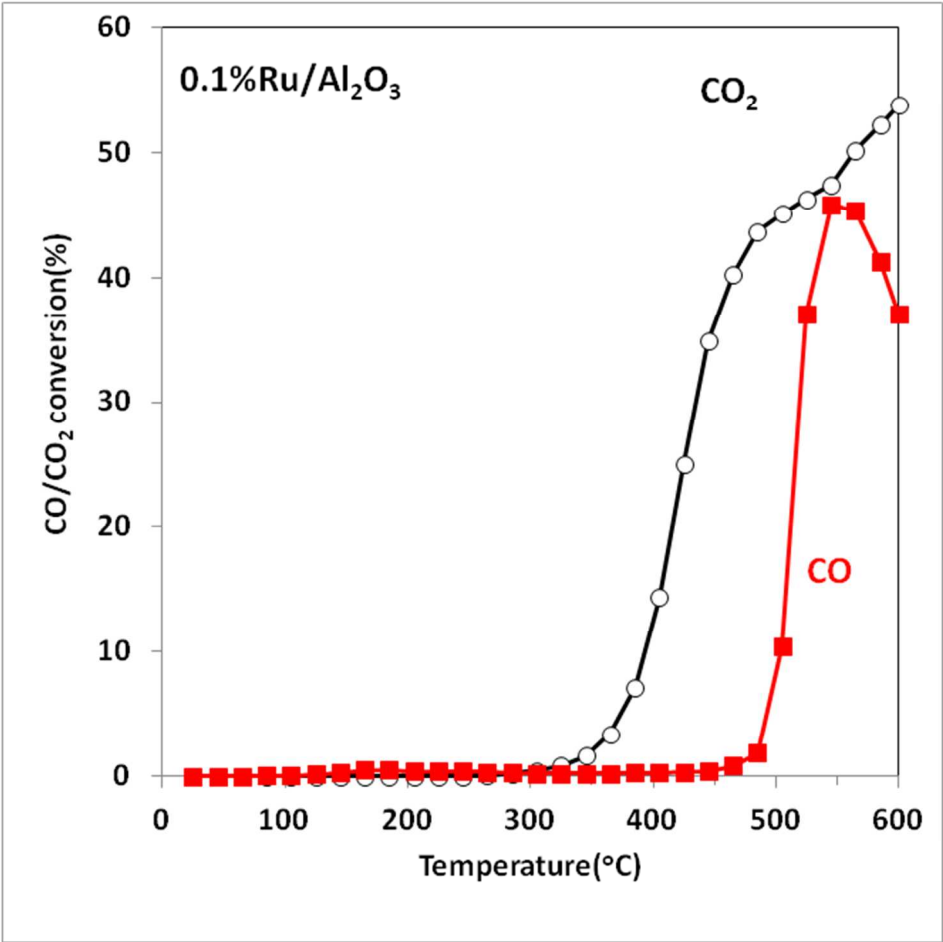


Figure 6



TOC:

